Stability of Metallic Dimers on the Si(001) Surface

Inder P. Batra
IBM Research Division, Almaden Research Center, K33/801, 650 Harry Road, San Jose, California 95120-6099
(Received 25 April 1989)

Total-energy calculations for prototype metals like Al and Ga on Si(001) 2×2, 2×1, and 1×2 surfaces predict important new structures and provide their bond strengths. It is estimated that at about 0.5-monolayer coverage the surface reconstruction is lifted and metallic dimers become stable. New low-energy Peierls-distorted structures provide a more natural explanation for the 5×2 and 3×2 LEED patterns. The reported trend in desorption energy as a function of coverage is reproduced, but more importantly specific conditions for observing this trend are obtained.

PACS numbers: 73.20.At, 71.30.+h, 73.20.Hb, 73.40.Ns

Coverage-dependent adsorption of metals on semiconductors has applications in several areas of condensed matter physics besides growth, Schottky-barrier formation, and metallization, in general.[1] The atomic and the resultant electronic structure of metal-semiconductor systems is a challenging endeavor at the first-principles level. This is not difficult to appreciate considering that the atomic reconstruction of Si itself has involved efforts extending over several decades. The adsorption of metals on Si can lead to removal of reconstruction of the substrate or it may lead to some other complex rearrangements which are clearly metal-coverage dependent. It therefore stands to reason that our knowledge at this point is limited to a handful of systems. One example is the work by Northrup,[2] who first predicted theoretically that upon substrate rearrangement Al atoms tend to favor T_4 sites on Si(111) as opposed to H_3 if the substrate if held in the ideal position. Another significant theoretical calculation by Zhang, Cohen, and Louie[3] demonstrated that Al removes the relaxation of GaAs(110) at a certain coverage.

In this Letter we take a significant step towards providing the atomic structure of metals like Al and Ga on the Si(001) 2×1 surface at initial coverages. Extensive total-energy calculations are presented for Al. Some sample calculations for Ga suggest that the results can be readily generalized to Ga and In as well. The coverage-dependent growth of Ga on Si(001) 2×1 is also important because of major technological interest in growing[4] GaAs on Si for optoelectronic devices. Gallium, indium, and arsenic overlayers on Si(001) have been studied experimentally[5-9] and the structures at all coverages have been explained by postulating metallic dimer formation.[6,7] For As dimers, geometric parameters have been reported[9] only for $\theta=2$ on ideal Si(001). Incidentally, one monolayer (1 ML $=6.78\times10^{14}$ adsorbates/cm^2) corresponds to $\theta=2$ in our definition, θ being the number of adsorbate atoms per 2×1 surface unit cell. Our calculations support the formation of metal dimers at $\theta=2$, which have also recently been observed in scanning tunneling microscopy experiments.[10] The origin of these dimers is explained in terms of Peierls distortion of a nearly one-dimensional metallic system. The metal dimerization opens up a gap at E_F and leads to an energetically more favorable state. Our calculations also predict other hitherto unreported low-energy structures. These new structures hold the key to understanding the 5×2, 3×2, and 2×2 LEED patterns.[5-7] Also, by comparing adsorption energies of various structures, we conclude that the substrate reconstruction is lifted at about 0.5 ML, in accord with recent data[6] on Ga. Finally, the observed decrease[6] in metal desorption energy as a function of coverage is explained. A condition is stated under which one would observe an opposite trend.

All our calculations are based on an extensive set of *ab initio* total-energy electronic structure and force calculations performed within the repeating slab geometry. We use the standard self-consistent-field pseudopotential method in the momentum-space representation[11] with norm-conserving nonlocal core potentials.[12] To arrive at definitive conclusions it was necessary to perform a large number of calculations for 1×1, 2×1, 1×2, and 2×2 unit cells. The calculational parameters were systematically increased [for example, the number of plane waves (PW) was varied from 700 to 1500] to ensure that computed energy differences had sufficiently converged to give reliable optimal structures. Since an empirical interaction potential for the metal-semiconductor system is not known, it is intractable to employ finite-temperature structural optimization techniques for Al-Si(001) especially for the 2×2 cells. Wherever possible, we used the LEED observations[5-7] to guide us in choosing the initial structures.

There is convincing evidence[5-7] that Ga and In at $\theta=1$ give rise to $\frac{1}{2},\frac{1}{2}$ LEED patterns. Consequently, one must work with a basic unit cell which has twice the area [see Fig. 1(a)] of the conventional[13] 2×1 surface cell. We have chosen the Si-atom dimerization direction ([110]) along the x axis and used the atomic positions given by Abraham and Batra.[13] Within the 2×2 cell one must accommodate two metal atoms at energetically optimal sites. Of the many structural models studied by us

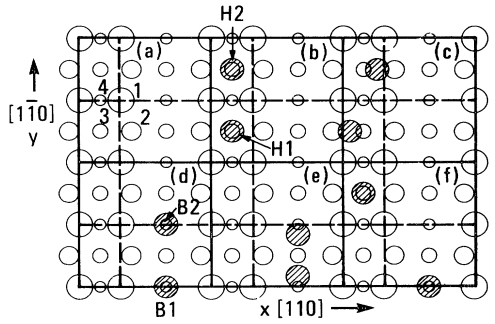

FIG. 1. Surface unit cells. (a) Reconstructed Si(001) 2×2; (b)–(f) descriptions of the configurations of Al overlayers at $\theta=1$. Cross-hatched and empty circles denote Al and Si atoms, respectively. Numerals by the circles in (a) indicate Si atomic layers.

at $\theta=1$ some significant ones are shown in Figs. 1(b)–1(f). The hollow sites $H1(4,2,1)$ and $H2(4,2,1)$ (the numbers in parentheses give the number of Si neighbors in the first three Si layers around an adsorption site) above the third layer of Si are quasihexagonal sites as shown in Fig. 1(b). This model is designated as $R(H1/H2)$, where R indicates that the substrate is reconstructed. Letter I shall be used for the ideal Si surface. Another structural model, called $R_x(H1/H2)$, shown in Fig. 1(c), consists of moving the metal atoms by $\pm\Delta x$ and is an important new low-energy structure. In long-bridge sites, $B1(2,4,2)$ and $B2(2,4,2)$, the adsorbates are placed above fourth-layer Si atoms. This is shown in Fig. 1(d) and is called $R(B1/B2)$. A significant variation of this model, $R_d(B1/B2)$, shown in Fig. 1(e), consists of moving the metal atoms by $\pm\Delta y$ to create metal dimers along the y direction ([1$\bar{1}$0]). The model $R(H2/B1)$ shown in Fig. 1(f) consists of occupying long-bridge and a quasihexagonal sites simultaneously. Other possible sites were ruled out either from preliminary energy calculations or on physical grounds.

TABLE I. Calculated relative binding energies ΔE_b (in eV) measured with respect to Al_2 adsorption at bridge sites [see Fig. 1(d)] on the ideal Si(001) 2×2 surface at $\theta=1$. The optimized vertical heights, h, and the nearest-neighbor d(Al-Al) and d(Si-Al) distances are given (in Å) for several models (R for Si dimer reconstruction and I for ideal substrate). More negative values for ΔE_b correspond to energetically more favorable configurations.

Model	ΔE_b	h	d(Al-Al)	d(Si-Al)
$R(H2/B1)$	−0.1	0.74	6.94	2.59
$R(H1/H2)$	−1.2	1.27	3.84	2.59
$R_x(H1/H2)$	−1.4	1.38	4.15	2.40
$R(B1/B2)$	−0.4	0.74	3.84	2.74
$R_d(B1/B2)$	−1.3	0.74	2.57	2.81
$I_d(B1/B2)$	−1.6	1.27	2.57	2.39
$I(B1/B2)$	0.0	1.27	3.84	2.30

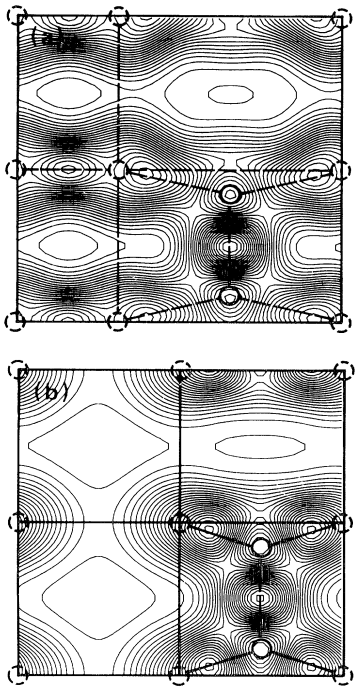

FIG. 2. Charge-density plots in the x-y plane passing through the Al overlayer for (a) model $R_d(B1/B2)$ shown in Fig. 1(e), and (b) where the substrate is in the ideal structure $[I_d(B1/B2)]$. Maximum charge-density values are 0.056 and 0.052 with contour spacings of $0.002e/(\text{a.u.})^3$. The positions of Si and Al atoms are indicated by dotted and open circles, respectively. The dotted circles show that Si atoms are not in this plane.

The binding energies for optimized metal layers on various substrates at $\theta=1$ are presented in Table I. The three low-lying minimum-energy structures are $I_d(B1/B2)$, $R_x(H1/H2)$, and $R_d(B1/B2)$, with $R(H1/H2)$ being a close fourth (saddle-point) structure. Tabulated values are for 1200 PW; the crucial values were checked by increasing the number of PW to 1500. Full atomic optimization, to be reported subsequently, confirmed the three to be the low-lying competitive structures. It is perhaps expected or can be anticipated from bonding and Peierls-instability type of arguments that a trivalent atom like Al can lower its energy by forming Al dimers along the y direction on both ideal as well as reconstructed Si(001) 2×2 surfaces. This explains why the model shown in Fig. 1(e) has lower energy than the one shown in Fig. 1(d). One important fact that emerges is that the Si-Al bond energy is stronger (by $\delta E_1=0.8$ eV) on the ideal surface as compared to the reconstructed surface. This follows from the values in Table I combined with our calculated Si-Si dimer bond energy, $E_d=1.8$ eV. Although the $R(B1/B2)$ model is 0.4 eV more stable than $I(B1/B2)$, we have broken two Si dimers at a cost of 3.6 eV in going from $R(B1/B2)$ to $I(B1/B2)$. Since the net loss is only 0.4 eV, it therefore follows that two

Al atoms which form four Si-Al bonds on the ideal surface have reconvered 3.2 eV (or 0.8 eV per Si-Al bond).

Another significant result that follows by comparing the energies of $R(B1/B2)$ and $R_d(B1/B2)$ is that on the reconstructed Si surface, Al dimerization leads to an energy lowering of 0.9 eV per Al dimer. A much stronger ($\sim$1.6 eV) Al-Al bond results upon Al dimerization on the ideal surface as can be seen from the relative energies of $I(B1/B2)$ and $I_d(B1/B2)$. Thus the Al-Al dimer bond on the ideal surface is more stable by $\delta E_2 = 0.7$ eV. An explanation as to why Al dimerization on the ideal surface leads to a stronger bond is due to the fact that the Al-Al bond of 2.57 Å is more naturally achieved on the ideal surface while retaining the Si-Al bond length at a desirable value of 2.4 Å. Notice that 2.57 Å is about 10% shorter than the bulk Al bond length. This is what Al prefers[14] when it loses a complement of its full shell. On the reconstructed surface Si-Al bond length becomes 2.8 Å in order to achieve d(Al-Al) = 2.57 Å, leading to a lower overall adsorption energy. This point also comes across clearly from an examination of the planar $(x\text{-}y)$ charge-density plots in Fig. 2 through the Al plane for adsorption on ideal and reconstructed surfaces. Bonds are distorted considerably on the reconstructed surface.

One novel low-energy structure, $R_x(H1/H2)$ [Fig. 1(c)], predicted by our calculation has to do with another type of Peierls distortion[15] of the Al atoms adsorbed at the H sites. The four-lobe cloverleaf bond formation (with all Si-Al bond lengths of 2.59 Å) shown in Fig. 3(a) makes the adsorption at H sites very competitive with Al-dimer formation at the B sites. In fact, the adsorption at the H sites is only 0.1 eV less stable compared to the B sites where Al-Al dimerization has already taken place. No Al-Al dimerization is possible at the H sites; a strong repulsive barrier was found in our calculation. However, a displacement of Al atoms along the x direction (calculated $\Delta x = 0.8$ Å) produces a lower-energy configuration due the formation of four strong Si-Al bonds of length 2.4 Å. This bond length is quite close to what Al achieved upon dimerization on the ideal surface. Those bonds, as we noted before, are more stable by 0.8 eV. The Δx distortion is not a band-gap-opening transition because the system is more nearly two dimensional; instead it is a bond-optimization rearrangement. Furthermore, as can be seen by comparing the charge-density plots in Fig. 3(a) with Fig. 3(b), the Si dangling bonds have to pay a smaller bond-rotation energy cost for the latter.

At $\theta = 2$ our calculations project that dimerized Al atoms on an ideal Si surface is the optimum model. The optimized values for this model are similar to those given in Table I for the $I_d(B1/B2)$ model. Adsorption on H sites or mixed H and B sites was ruled out by our calculations. The fractional-order spots[6] in LEED at $\theta = 2$ then originate due to the 1×2 structure which the Al dimers adopt after removing the Si reconstruction. These

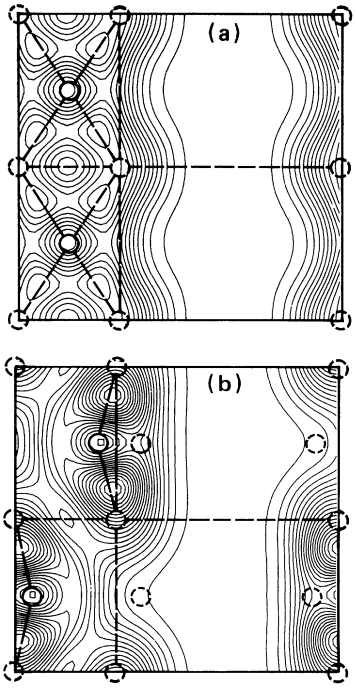

FIG. 3. Charge-density plots in the x-y plane passing through the Al overlayer (a) for model $R(H1/H2)$ shown in Fig. 1(b) and (b) for model $R_x(H1/H2)$ in Fig. 1(c). Maximum charge-density values are 0.029 and 0.042 with contour spacings of $0.002e/(\text{a.u.})^3$.

results are similar to those reported[9] for As. For Ga dimers, our calculation gives $h = 1.1$ Å and d(Ga-Ga) = 2.39 Å. These values are slightly lower than the corresponding values for Al, in agreement with the notion that the Ga atomic radius is somewhat smaller than that of Al.

The values given in Table I enable us to estimate the critical coverage, θ_c, at which the surface relaxes back to its ideal bulk truncated structure. There is a competition between forming Al-Si bonds at the reconstructed surface (which lowers the total energy) and breaking Si-Si dimer bonds (which raises the energy) with subsequent lowering of the total energy due to formation of more favorable bonds at the ideal surface. A simple energy-balance argument then gives $\theta_c = 2E_d/\Delta E$, where E_d is the Si-Si dimer bond energy on a reconstructed surface (1.8 eV) and $\Delta E = 4\delta E_1 + \delta E_2$ is the excess Al_2 binding energy on the ideal as compared to the reconstructed Si(001) 2×2 surface. Our calculations give $\Delta E = 3.9$ eV and hence $\theta_c = 0.92$ (or 0.46 ML). In view of the modest number of PW used in the calculations, the critical value may have an uncertainty of ± 0.1 ML. A recent experiment[6] for Ga on Si(001) finds that the reconstruction is lifted at $\theta \simeq 1$, and is in conformity with our estimate for the Al/Si system.

It has been observed experimentally that the desorp-

tion energy for Ga decreases by 0.6 eV as the coverage increases towards 1 ML. Our total-energy calculations performed on clean and adsorbate-covered surfaces give for Al a decrease of desorption energy[16] 0.6–0.7 eV/Al atom (depending on the computational parameters) from between $\theta = 1$ and 2 provided the substrate geometry is not significantly altered at the two coverages. If the low-coverage adsorption is referred to the reconstructed surface then the Al adsorption energy is in fact lower at the low coverage and the opposite trend would be observed.

An intriguing 5×2 LEED pattern has sometimes been reported[5,6] for the Ga/Si system. It has been explained by packing metal dimers of model $R_d(B1/B2)$ [see Fig. 1(e)] with the appropriate density. Since 5×2 patterns are not frequently observed,[5,6] we find it more natural to explain the 5×2 structure as arising from metal atoms being in two competitive low-energy structures $R_x(H1/H2)$ and $R_d(B1/B2)$. The relative rarity of this structure is connected with the fact that when one Al atom is present around an H site, a second Al atom has no strong affinity to be in the adjacent H site since no metal dimerization is possible. This is different from the case of the metal atom being in a B site where a second Al atom can readily lead to a metallic dimer structure. The 3×2 structure can arise equally well by packing Al_2 in the $R_x(H1/H2)$ or $R_d(B1/B2)$ structure by leaving one 2×1 cell empty between every 2×2 cell.

In conclusion, the coverage-dependent calculations presented here give values for important binding energies. Our calculated value for the critical coverage, at which the surface reconstruction is lifted, is in accord with the available data. The relevance of these results to the Fermi-level pinning and Schottky-barrier problem shall be explored in a complete paper. We have also provided new low-energy Peierls-distorted structures which are capable of explaining observed LEED patterns.

[1]See, for example, I. P. Batra, in *Metallization and Metal-Semiconductor Interfaces,* NATO Advanced Study Institutes Series Vol. 195 (Plenum, New York, 1989), p. 1.

[2]J. E. Northrup, Phys. Rev. Lett. **53**, 683 (1984).

[3]S. B. Zhang, M. L. Cohen, and S. G. Louie, Phys. Rev. B **34**, 768 (1986).

[4]See, for example, H. Kroemer, J. Cryst. Growth **81**, 193 (1987); J. R. Patel, P. E. Freeland, M. S. Hybertsen, and D. C. Jacobson, Phys. Rev. Lett. **59**, 2180 (1987); E. Kaxiras, O. L. Alerhand, J. D. Joannopoulos, and G. W. Turner, Phys. Rev. Lett. **62**, 2484 (1989).

[5]T. Sakamoto and H. Kawanami, Surf. Sci. **111**, 177 (1981).

[6]B. Bourguignon, K. L. Carleton, and S. R. Leone, Surf. Sci. **204**, 455 (1988).

[7]J. Knall, J.-E. Sundgren, G. V. Hansson, and J. E. Greene, Surf. Sci. **166**, 513 (1986).

[8]R. I. G. Uhrberg, R. D. Bringans, R. Z. Bachrach, and J. E. Northrup, Phys. Rev. Lett. **56**, 520 (1986).

[9]R. I. G. Uhrberg, R. D. Bringans, R. Z. Bachrach, and J. E. Northrup, J. Vac. Sci. Technol. A **4**, 1259 (1986).

[10]J. Nogami, S. Park, and C. F. Quate, Appl. Phys. Lett. **53**, 2086 (1988); D. M. Chen, J. A. Golovchenko, P. Bedrossian, and K. Mortense, Phys. Rev. Lett. **61**, 2867 (1988).

[11]J. Ihm, A. Zunger, and M. L. Cohen, J. Phys. C **12**, 4409 (1979); K. C. Pandey, Phys. Rev. Lett. **49**, 223 (1982).

[12]C. B. Bachelet, D. R. Hamann, and M. Schluter, Phys. Rev. B **26**, 419 (1982).

[13]M. T. Yin and M. L. Cohen, Phys. Rev. B **24**, 2303 (1981); F. F. Abraham and I. P. Batra, Surf. Sci. **163**, L752 (1985).

[14]I. P. Batra, J. Vac. Sci. Technol. A **3**, 1603 (1985).

[15]Y. Ling, A. J. Freeman, and B. Delley, Phys. Rev. B **39**, 10144 (1989).

[16]S. Ciraci and I. P. Batra, Phys. Rev. B **37**, 2955 (1988).